Atmospheric Environment 292 (2023) 119416

Contents lists available at ScienceDirect

Atmospheric Environment

journal homepage: www.elsevier.com/locate/atmosenv

Source attribution of particulate matter in Berlin

Joscha Pültz [a,*], Sabine Banzhaf [a], Markus Thürkow [a], Richard Kranenburg [b], Martijn Schaap [a,b]

[a] Institute for Meteorology, Freie Universität Berlin, Carl-Heinrich-Becker-Weg 6-10, 12165, Berlin, Germany
[b] TNO, Netherlands Organisation for Applied Research, Climate, Air and Sustainability Division, 3508 TA, Utrecht, the Netherlands

HIGHLIGHTS

- A sectoral and regional source attribution for Berlin was performed.
- The most important source sectors for PM are households and industry & energy.
- Transboundary contributions are smaller than domestic contributions.
- Missing resuspension processes may explain the underestimation of the coarse mode.

ARTICLE INFO

Keywords:
Chemistry-transport model
Source attribution
Coarse mode
Urban increment
Lenschow-approach

ABSTRACT

The exposure to ambient particulate matter in metropolitan areas is a major health problem. A prerequisite for formulating effective mitigation strategies it to understand the origin of particulate matter in terms of source regions and sectors. We performed a source attribution of particulate matter (PM) for the Berlin agglomeration area covering the period from 2016 to 2018 using the LOTOS-EUROS chemistry transport model. The (3 year-) mean modelled urban background $PM_{2.5}$ concentration (10.4 μg/m^3) is largely explained by households (3.2 μg/m^3) and industry & energy (2.0 μg/m^3), while the remaining source sectors contribute the other half. The modelled annual mean urban increment for $PM_{2.5}$ is mainly attributed to households (1.6 μg/m^3) and traffic (0.5 μg/m^3). With respect to its relative shares the PM_{10} source attribution looks similar to that of $PM_{2.5}$ throughout the year, but with enhanced natural contributions. From a geographical perspective the main source area for the $PM_{2.5}$ in Berlin is Germany (5.1 μg/m^3) itself, followed by the contributions from transboundary transport (3.4 μg/m^3). The German sources could be further split into Berlin (2.6 μg/m^3), Brandenburg (0.7 μg/m^3) and remaining states of Germany (1.8 μg/m^3). About one third of the foreign shares can be attributed to Germany's neighbouring countries Poland and Czech Republic. During episodes these contributions can significantly differ, e.g. in February 2017 the Polish contribution is about 1/3rd. The sectoral contributions agree with previous findings except that our study indicates lower contributions for traffic. The model's underestimation of total PM is largely caused by an underestimation of the coarse mode PM. Both the coarse mode urban increment as well as the regional background concentrations are underestimated by the model, especially during summer. We suggest that the enhanced coarse material (in the city) during warm seasons is predominated by (road) resuspension processes which need more of our attention to further improve our models.

1. Introduction

Air pollution remains the single largest environmental health risk in Europe according to the World Health Organization (World Health Organization Regional Office for Europe, 2015). The adverse health effects of air pollution are dominated by exposure to particulate matter (PM) (Boldo et al., 2006; Brook et al., 2010; Costa et al., 2014). Harmful effects as cardiovascular and respiratory diseases, can ultimately lead to premature death (Newby et al., 2015). In Europe, the average reduction in life expectancy due to fine particulate matter ($PM_{2.5}$) is estimated in the order of 8–10 months (Boldo et al., 2006; Brook et al., 2010). Although a large proportion of the European population is exposed to levels above the WHO air quality guidelines, current EU limit values for PM in Europe are exceeded to a limited extent. Exceedances of the daily limit value for PM_{10} in Germany are measured particularly at monitoring sites close to traffic and industry in large conurbations

* Corresponding author.
E-mail address: joscha.pueltz@met.fu-berlin.de (J. Pültz).

https://doi.org/10.1016/j.atmosenv.2022.119416
Received 28 September 2021; Received in revised form 29 August 2022; Accepted 29 September 2022
Available online 4 October 2022

(Umweltbundesamt, 2019). To protect citizens from the negative effects of air pollution and to bring PM concentration levels below the limit value, it is necessary to elaborate effective mitigation strategies. In order to develop effective mitigation strategies, it is crucial to understand which sources contribute to the particulate matter exposure (Pandolfi et al., 2020) and which mitigation options have the largest impact, especially for high concentration episodes (Belis et al., 2020). A prerequisite is that the modelling systems used for developing mitigation strategies explain the observed levels and variability in particulate matter well.

PM encompasses a wide range of particle types, regarding size (coarse: PM_{10} and fine: $PM_{2.5}$), chemical composition (e.g., mineral dust, combustion particles, sea salt, secondary inorganic aerosol, secondary organic aerosol, metals), and sources (e.g., natural, traffic, industry, domestic households, secondary processes) (Putaud et al., 2004). Its contributions depend on local sources as well as its location with respect to source regions located further away and vary strongly depending on synoptic meteorological conditions and season (Lenschow et al., 2001; Mues et al., 2012; Fuzzi et al., 2015; van Pinxteren et al., 2019). Sources of PM in urban areas are traffic, domestic heating, cooking, construction sites, industries, power generation or mineral dust (e.g., Querol et al., 2004). Long-range transport prevalent as the rural background is normally dominated by contributions from combustion processes and secondary aerosols, e.g. ammonium nitrate and sulphate (van Pinxteren et al., 2019). Whereas PM episodes may be driven by a local or regional build-up of pollution (e.g. Banzhaf et al., 2013), the urban concentration levels during episodes may also be largely controlled by long range transport to a city (Beekmann et al., 2015). Hence, many cities are unable to meet target levels for air pollutants through local action alone (van Pinxteren et al., 2019). To identify the origin and quantify both natural and anthropogenic source contributions to urban PM levels is an important task.

There are various methodologies to identify and apportion PM to different sources. Statistical data analyses of observations are often used. The Lenschow approach is a simple method, in which urban increments that correspond to the concentration difference between the urban and the regional locations are calculated (Lenschow et al., 2001). The increment is assumed to be the impact of a city on its own air pollution. The main advantage is a simplified data treatment with low impact of mathematical artefacts (Viana et al., 2008). A weakness of the method is that the assumption of the independency of the two locations may not be fulfilled (Thunis, 2018). A further helpful method is to apply air trajectories to identify source regions which can be long-range or trans-boundary (e.g., Potier et al., 2019). Positive Matrix Factorization (PMF) attempt to apportion the sources based on observations (internal correlations) at the receptor site alone. A very distinct advantage is the detailed source profiles PMF provides. This method is often used for analysis because detailed prior knowledge of the sources and source profiles is not required and software to perform this type of analysis is widely available (Viana et al., 2008). Normally, receptor modelling studies can distinguish a limited number of broad source categories. An essential disadvantage is the inability to provide a source apportionment for secondary components. Furthermore, these experimental approaches do not yield information on the geographical origin. Finally, the required chemical analyses are expensive leading to many applications in campaigns and a limited availability of long time series (Hendriks et al., 2013).

Complementary to methods based on observations, deterministic Eulerian Chemistry Transport Models (CTMs) are widely used to obtain more detailed information on air pollution and its origins. By involving atmospheric process descriptions and emission inventories they provide calculations of the evolution of the air pollution situation across a region (Baklanov et al., 2014). To gain insights in source contributions, several methodologies have been used in the past. The simplest approach is the brute force (BF) method, in which the emissions of the source sectors under investigation are reduced and compared to a base case simulation (e.g., Belis et al., 2020; Banzhaf et al., 2013). Through extrapolation of the resulting concentration changes the source sector contribution can be estimated. For inert compounds these approaches provide equivalent results (Thunis et al., 2019). It has to be highlighted that the BF method and labelling approach lead to different source attribution (SA) results due to non-linear chemical effects, such as for the formation of secondary inorganic aerosol (e.g. Thunis et al., 2020). The main advantage of the BF methodology is that it directly provides information on the effectiveness of potential measures. However, by upscaling the impacts one may over- or underestimate the baseline concentration, which becomes a larger issue in case of situation with a limiting formation process and on short time scales (Li et al., 2014; Thunis et al., 2015; Pommier et al., 2020; Thürkow et al., 2022). Moreover, in case of a limitation in the formation small sized emission sources may be given a zero or low impact and thus may be overlooked as a relevant contributor (Thunis et al., 2020; Thürkow et al., 2022). In this situation detailing a large sector as traffic further into subsectors may lead to the situation that the sum of the sub-sectors is away from the sector estimate (Clappier et al., 2017). This may be amplified in case also the spatial and temporal variability are different per subsector. Also, the resulting source apportionment is sensitive to the reduction percentage applied (Napelenok et al., 2006). Due to the intrinsic assumption that each molecule has the same chance of reaction adopted in the labelling implementation these effects do not occur. The resulting source apportionment is additive and complete, but does not per se indicate the effectiveness. Note that above mentioned concerns disappear when the brute force apportionment is performed within its limits of applicability, i.e. for a limited range of emission reduction strengths (Clappier et al., 2017). Hence, we see a labelling based source apportionment as a valuable first step to identify and quantify the relevant sectors to be further addressed in brute force calculations to determine efficiency of potential measures. This is further supported by the fact that the labelling strategy is more computationally efficient enabling to detail a larger number of source contributions than normally feasible in brute force studies (Belis et al., 2020). Methods like Decoupled Direct Method (DDM; Dunker et al., 2002; Zhang et al., 2012) at least partly, solve this computational burden for brute force approaches. Although first operational applications are becoming available (Pommier et al., 2020), the experience using such model-based source apportionment is still relatively scarce in Europe.

In this paper, we apply the LOTOS-EUROS CTM version 2.1 to identify the most relevant sources with regards to their contributions of PM for the German capital Berlin. The model was applied to a 3-year time frame from January 2016 to December 2018 for which we quantified the urban sector contributions as well as the long-range transport contributions using a labelling approach. As CTMs do not fully explain the observed PM concentration and variability (e.g., Belis et al., 2020), special emphasis is put on the identification of shortcomings. For comparison of modelled urban increments to observational data we adopted the Lenschow-approach (Lenschow et al., 2001). Finally, we discuss our findings in comparison to earlier studies oriented at source attribution for Berlin or model-based source apportionment.

2. Methodology

2.1. Chemical transport modelling

In this paper, we apply the LOTOS-EUROS CTM version 2.1 to investigate the origin of PM in Berlin during a 3-year time frame from January 2016 to December 2018. LOTOS-EUROS is a 3D chemistry transport model (CTM) developed by the Netherlands Organization for Applied Scientific Research (TNO) and partners including the Freie Universität Berlin (FUB, Germany). The LOTOS-EUROS CTM is an Eulerian grid model, which was originally developed to simulate ozone and smog concentration levels in the lower troposphere in Europe. In the vertical a mixed-layer approach is applied (Manders et al., 2017) using 5

terrain following layers extending up to 5 km above sea level (orography). In this study we set up a European domain (D1) with a horizontal resolution of 0.5° (longitude) and 0.25° (latitude) corresponding to about 28 × 32 km^2. An increased resolution is obtained for a nested domain (D2) covering Germany and Poland with 0.125° (longitude) and 0.0625° (latitude), approximately 7 × 8 km^2. Poland was included in the high-resolution domain as the transboundary component is of specific interest for the local policy (details see Fig. 1). The model describes the fate of anthropogenic primary particulate matter (ppm), including a separation of elemental carbon (EC) and organic material (POM). The formation of secondary inorganic aerosol (SO_4, NO_3 and NH_4) from its precursor gases and the emissions of (semi-) natural emissions of sea salt and mineral dust are also described. The model follows a bulk approach for the fine (f) and coarse (c) aerosol mode (a). The total particulate matter mass is computed from the individual model compounds:

$$PM_{2.5} = SO_{4af} + NH_{4af} + NO_{3af} + EC_f + POM_f + PPM_f + 3.26 * Na_f + Dust_f \quad (1)$$

$$PM_{10} = PM_{2.5} + NO_{3ac} + POM_c + PPM_c + 3.26 * Na_c + Dust_c \quad (2)$$

The LOTOS-EUROS model adopts sodium as the preserved sea salt tracer, and its concentration is multiplied by a factor 3.26 to arrive at the total sea salt contribution.

Meteorological data were taken from ECMWF (European Centre for Medium-range Weather Forecasts). The model configuration, except the domain definition, resembles the set-up used within the regional ensemble of the Copernicus Atmospheric Monitoring Service (CAMS). Within CAMS LOTOS-EUROS is applied to provide operational air quality forecasts and analyses for Europe (Marécal et al., 2015) including source apportionment information for major cities (Pommier et al., 2020). For a more detailed description of LOTOS-EUROS we refer to Manders et al. (2017).

The gas-phase chemistry is described by the TNO CBM-IV scheme, a modified version based on the development by Whitten et al. (1980). Aerosol chemistry is formulated within the thermodynamic equilibrium module ISORROPIA2 (Fountoukis and Nenes, 2007). Coarse mode nitrate formation is modelled dynamically through a surface reaction on sea salt. Sea salt emissions are parameterized using two schemes for the fine and coarse mode (Mårtensson et al., 2003; Monahan et al., 1986). Resuspended mineral dust from road-traffic is parameterized using constant emission factors and depends on the traffic intensity in the respective grid cell (Schaap et al., 2009). In a similar vein, the agricultural land management emissions are parameterized using constant emission factors per activity and are allocated over the months in which the activity typically occur (Schaap et al., 2009). Both sources are switched off in case of rain. Windblown dust is parameterized by sand blasting schemes (Manders et al., 2017), but normally do not impact Berlin. Forest fire emissions were taken from the CAMS global fire assimilation system (Kaiser et al., 2012). Dry deposition fluxes for reactive gases are calculated using the resistance approach as implemented in the DEPAC (Deposition of Acidifying Compounds) module (Wichink Kruit et al., 2012). Particle deposition follows the scheme of Zhang et al. (2001). Wet deposition is parameterized as described in Banzhaf et al. (2012). Secondary organic aerosol formation was neglected, as the VBS-module was not yet implemented in the source apportionment approach of the model.

The annual total emissions were based on the official country reporting to the UNECE and the EU for 2017. Except for Germany, emissions were gridded based on the CAMS reporting (Copernicus Atmospheric Monitoring System) database. For Germany, the gridded emissions were obtained from the GrETa system (GRETA – Gridding Emission Tool for ArcGIS v1.1; Schneider et al., 2016). The totals are apportioned to monthly, daily, and hourly amounts by sector-specific time factors. For CO and VOC temperature-dependent factors were used (Manders et al., 2017). The official emissions for residential wood combustion (RWC) were replaced by a scientific bottom-up inventory for Europe (Denier Van Der Gon et al., 2015). This contains a consistent set of emission factors for wood combustion and includes the impact of condensable material (Denier Van Der Gon et al., 2015). Overall, the RWC emissions in this study were by a factor of 2–3 higher than the officially reported. To incorporate the dependency of heating demand on temperature the temporal variability of RWC emissions was calculated using heating degree days. The heating degree demand was calculated relative to a reference temperature (18 °C). We used a fraction of 20%, for emissions not related to heating following Mues et al. (2014).

2.2. Source attribution

To assess the contribution of different source sectors and regions we applied the source apportionment module implemented in the LOTOS-EUROS CTM (Hendriks et al., 2013; Kranenburg et al., 2013a). Through a labelling procedure the origin of species is traced through the process descriptions for the transport and chemical reactions (Kranenburg et al., 2013a). The labelling approach works for primary, inert aerosol tracers and chemically tracers in which a C, N (oxidized and reduced) or S atom is conserved. The validation of this module was done in (Kranenburg et al., 2013b) in dedicated experiments. The module was applied to PM (episodes) (Hendriks et al., 2013, 2015; Timmermans et al., 2017, 2020) and nitrogen oxides (Curier et al., 2014; Schaap et al.,

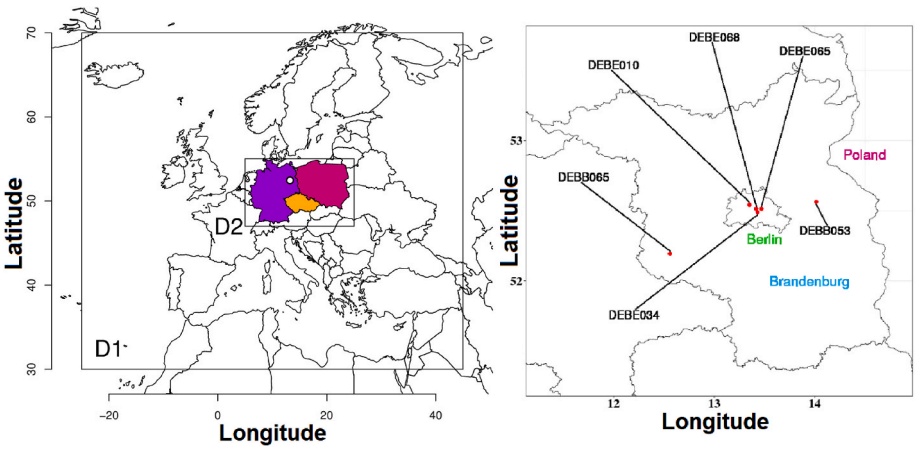

Fig. 1. The D1 domain for Europe and therein the D2 domain for Germany/Poland/Czech Republic, the position of Berlin is indicated with a white circle (left). Illustration of the measurement locations in Berlin and the surrounding federal state of Brandenburg (right). The colours correspond to the related labels. (For interpretation of the references to colour in this figure legend, the reader is referred to the Web version of this article.)

2013). The source attribution for ammonium nitrate is calculated as a weighted mean of the source sectors contributing to the reduced and oxidized N-atom (in i.e., ammonium and nitrate) on a molar basis (Hendriks et al., 2013).

We defined 32 combinations of sectors and regions to be tracked. The 5 sectors we considered are the main source sectors for particulate matter (traffic, households, industry & energy, agriculture) and all remaining sectors combined as rest. To quantify the urban, regional, domestic, and transboundary contributions we separated 6 geographic regions: Berlin, Brandenburg, Rest of Germany, Poland, Czech Republic and all remaining countries as "other countries". In addition, the natural and boundary (incl. initial) conditions were traced (see Table 1).

2.3. Monitoring data

The present work focuses on a dataset containing daily PM_{10} and $PM_{2.5}$ mass concentrations for 6 selected air quality monitoring stations of the federal states of Berlin (4) and Brandenburg (2). For comparison reasons one urban traffic station is included additionally. The data were provided by the German Federal Environmental Agency (Umweltbundesamt, UBA) and the Senat of Berlin. Classifications, geographic coordinates, component, and short names of the measurement stations are listed in Table 2.

The observed data provides no information about the source region and/or the source sectors. This leads to the Lenschow approach, where rural and urban stations are selected and can be investigated separately and/or in a combined manner. As the approach can be also applied for modelled data, the modelled spatial gradient can be compared to the measured spatial gradient. Statistical indicators for the model performance were calculated in a common way (e.g., RMSE, BIAS, MEAN). For the correlation coefficient the Pearson correlation was used. When the spatial mean of a specific station type was calculated, the daily mean values were used. Suburban sites pose a challenge to the model, as the stations are located close to the city border. Grid cells which include these stations may be affected by substantial urban emissions leading to an overestimation of the rural to suburban increment. Hence, we mainly focus our analysis on the gradients between rural and urban background concentrations. The RB stations investigated are located west and east of the city, thus they show mean values for the RB, normally only upwind stations should be used. Meteorological data (such as wind and precipitation) were taken from the WMO station Berlin-Dahlem.

2.4. Investigation domain and periods

In this study we focus on the capital of Germany with around 4 million inhabitants. Berlin is located in the north-eastern part of Germany and surrounded by the federal state of Brandenburg. The closest neighbouring country, Poland, is about 60 km east of the city. The climate is characterized by westerlies, bringing maritime air towards Berlin while during some episodes preferably in midsummer and winter easterlies can prevail for several days up to weeks due to a continental high. For Berlin, the long-term annual precipitation amount of about 600 mm and mean temperatures of around 13 °C were observed. Prevailing wind directions are westerlies (~75%, NW to SW) and easterlies (~25%, NE to SE), with easterly wind directions mainly occurring during the winter season. Apart from a large power plant in the western part of the city, there is no major industry in the city or in the surrounding area.

Table 1
Labelled source regions (left) and source sectors (right).

Labelled regions	Labelled sectors
Berlin	Traffic
Brandenburg	Households
Rest of Germany	Industry & Energy
Poland	Agriculture
Czech Republic	Rest
Others	
Natural	Natural
Boundary	Boundary

3. Results

3.1. Observed levels for the investigation period

We provide an overview of the observed annual mean particulate matter mass concentration for 2016 to 2018 following the Lenschow's incremental approach (Fig. 2). The concentrations are classified by subcategories of the UBA measurement network for the rural background (RB, light grey), urban background (UB, dark grey) and urban traffic (UT, black). We provide the overview for PM_{10}, $PM_{2.5}$ and the coarse mode fraction (PM_{CO}, difference between PM_{10}-$PM_{2.5}$) for 2016 (left), 2017 (middle) and 2018 (right), separately. The share for the urban background is the difference between the concentration in the urban background and in the rural background and is called the urban increment. The same applies to the urban traffic and is accordingly referred to as the traffic increment.

The overall annual mean PM_{10} concentration at urban traffic sites was about 27–28 μg/m^3. The $PM_{2.5}$ level was about 17 μg/m^3, and the coarse mode was about 10 μg/m^3. The annual mean PM_{10} concentration in the urban background is in the range of 21–23 μg/m^3, while that of $PM_{2.5}$ is about 15 μg/m^3. Hence, the coarse mode contributes about 6–7 μg/m^3. For $PM_{2.5}$ the rural background (12–13 μg/m^3) is contributing about three quarters of the urban background concentrations, whereas for the coarse mode the relative contribution of the rural background is smaller, about 50% (3–4 μg/m^3). For PM_{10} the rural background concentration is measured to be about 15–17 μg/m^3. For $PM_{2.5}$ the urban increment (~3 μg/m^3) is slightly larger than the observed traffic increment (~2 μg/m^3). A low variability from year to year can be seen for annual-averaged levels of the $PM_{2.5}$ rural background, urban increment, and traffic increment. For the coarse mode, the urban background and traffic increments are similar (~3 μg/m^3 each).

Fig. 3 shows daily mean particulate matter mass concentrations averaged over all urban background stations from 2016 to 2018. The PM_{10} seasonal cycle reflects a pattern common to many cities in Europe. Largest PM_{10} concentrations are observed during wintertime, while smallest concentrations occur during summer. During episodes in winter, daily mean PM_{10} concentrations between 70 and 100 μg/m^3 were observed, whereas concentrations in summer hardly exceeded 40 μg/m^3. $PM_{2.5}$ shows a stronger seasonal cycle than PM_{10} as PM_{10} concentration episodes in winter consist mainly of fine material. The coarse mode shows the opposite seasonal cycle with maximum contributions during summer and early fall with enhanced fractions throughout the year at traffic and urban background stations.

Fig. 4 shows the observed PM_{10} daily concentrations for station DEBE034 with respect to the prevalent wind direction. During 2016 and 2017 the westerly wind directions (from NW to SW) dominate associated with low to medium PM_{10} concentrations (5–35 μg/m^3). In contrast, up to ¼ of the weather situations of the days with easterlies (from NE to SE) show concentrations above the daily limit value (up to more than 100 μg/m^3). These situations are often associated with cold temperatures, low wind speeds and stagnation conditions with shallow boundary layers in winter or spring. 2016 and 2017 can be considered as typical for the investigation period and correspond to the common climatological conditions. The meteorological conditions in 2018 on the other hand were atypical as easterlies were present for almost half of the year (~40%) and westerlies were less apparent (~45%). A prolonged drought characterized by low amounts of precipitation from mid-April until the end of the year occurred. Consequently, this year had the lowest annual precipitation (393 mm) on record since the beginning of measurements in Berlin/Brandenburg in 1881, whereas the long-term mean (1961–1990) is 557 mm (Deutscher Wetterdienst, 2020). During

Table 2
Measurement sites in Berlin and Brandenburg containing UBA-code, location, street, shortcut, longitude, latitude, characteristic, PM_{10} and $PM_{2.5}$ observed for 2018. B=Berlin, BB=Brandenburg; UT=Urban Traffic, UB=Urban Background, RB = Rural Background.

Station UBA-Code	Region & district	Address	Acronym	Geogr. latitude	Geogr. longitude	Type	PM_{10} [μg/m^3]	$PM_{2.5}$ [μg/m^3]
DEBE010	B Wedding	Amrumer Str./Limburger Str.	BEAMR	52.542744	13.349119	UB	21.43	15.07
DEBE034	B Neukölln	Nansenstraße 10	BENAN	52.489451	13.430844	UB	24.42	16.34
DEBE065	B Fried-richshain	Frankfurter Allee (86b)	BEFRA	52.514072	13.469931	UT	27.77	17.56
DEBE068	B Mitte	Brückenstr. 6	BEBRU	52.513606	13.418833	UB	22.74	15.44
DEBB053	BB Hasenholz	15377 Buckow	BBHAS	52.563835	14.015252	RB	19.33	14.11
DEBB065	BB Luette (Belzig)	Die hohe Heide/Feldstr.	BBLUE	52.194225	12.561389	RB	15.03	12.01

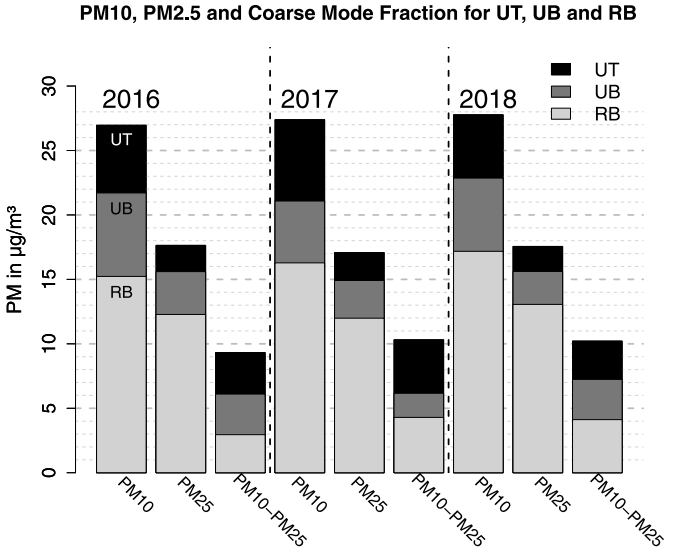

Fig. 2. Incremental Lenschow approach for observed data. For each UBA subcategory, the corresponding mean was calculated over the associated stations. Annual mean PM concentrations and increments (μg/m^3) between the rural background (RB, light grey), urban background (UB, dark grey) and urban traffic (UT, black) concentrations. For each year (2016, left; 2017, centre; 2018, right), a further subdivision into the three shares PM_{10} (left), $PM_{2.5}$ (centre) and the coarse mode fraction (PM_{10}-$PM_{2.5}$, right) was made.

2018 the easterly wind directions were associated with more moderate PM_{10} mass concentrations than the previous years as these easterlies occurred in the summer.

3.2. Model performance

To assess the robustness of the applied model to simulate PM concentrations, we compared the LOTOS-EUROS CTM results for Berlin to daily observations at UB and RB monitoring stations. Fig. 5 shows the observed and modelled $PM_{2.5}$ timeseries in the form of a bar chart and Fig. 6 shows the corresponding scatter plots. A selection of statistical measures (mean values, correlation, normalized RMSE and BIAS) for PM_{10}, $PM_{2.5}$ and PM_{CO} is presented in Table 3. While the model can reproduce a fair part of the temporal variability of $PM_{2.5}$ concentrations throughout the year, it is not able to catch major amplitudes. The underestimation is particularly visible in summer and early autumn while wintertime peaks are better reproduced. The model performs best during spring season in capturing concentration variability and amplitude. Also, the concentration level increase starting in early autumn is well reproduced by the model. During winter, the modelled $PM_{2.5}$ concentration averaged over all UB sites captures 75% of the observed (PM_{10}: 74%) concentration, while during summer only 57% (PM_{10}: 53%) is reproduced. The annual statistics show the underestimation of the model for PM in a negative BIAS at all stations (by 13–48% for the normalized BIAS). For all fractions - PM_{10}, $PM_{2.5}$ and PM_{CO} - the underestimation is more distinct at UB stations than at RB stations and generally larger during episodes. Furthermore, the correlation coefficient reveals that the model is better in capturing the variability in $PM_{2.5}$ concentrations than in those of PM_{10}. There is one RB station (DEBB065) which is slightly better simulated than all other stations, especially for $PM_{2.5}$.

When looking at the coarse mode material, modelled summertime concentration levels reflect only about fifty percent of those observed. In numbers, at RB (UB) stations the model captures 57% (47%) of the observed mass during summertime while during wintertime 132% (73%) of the observed mass at RB (UB) stations is modelled by LOTOS-EUROS. The mean observed summertime coarse mode urban increment of about 2.5 μg/m^3 is with 0.6 μg/m^3 considerably underestimated by the model. This is also valid for wintertime with an observed urban increment of 2.8 μg/m^3 compared to the modelled urban increment of 0.8 μg/m^3. The BIAS, correlation coefficients and normalized RMSE show that the coarse mode is largely underestimated, and that the temporal variability is poorly explained by the model.

The $PM_{2.5}$ and coarse mode urban increments (modelled and observed) are shown in Fig. 7. To suppress short-term fluctuations a

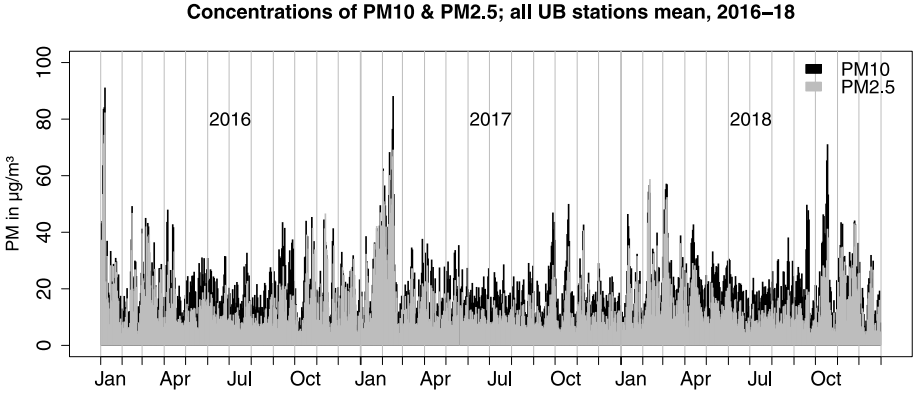

Fig. 3. PM_{10} and $PM_{2.5}$ mass concentration for the urban background (UB) stations (DEBE010, DEBE034, DEBE068) for 2016 to 2018. Observations (gravimetric) are shown as daily mean values with missing values are considered as no data available.

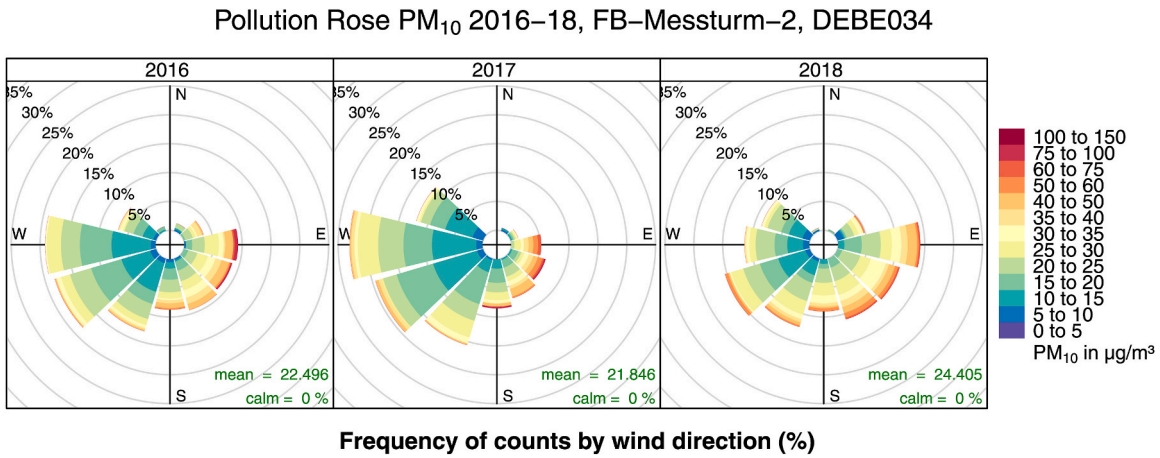

Fig. 4. Observed mass concentration for PM_{10} of the urban background (UB) station Berlin (DEBE034, Nansenstr.) for daily data (gravimetric) and wind measurement data from the wind gauge mast of the FU-Berlin for 2016 to 2018. The breaks for PM_{10} concentrations are not equally distributed, missing values are considered (this causes the sum of all contributions to be below 100% for some cases because of the missing values).

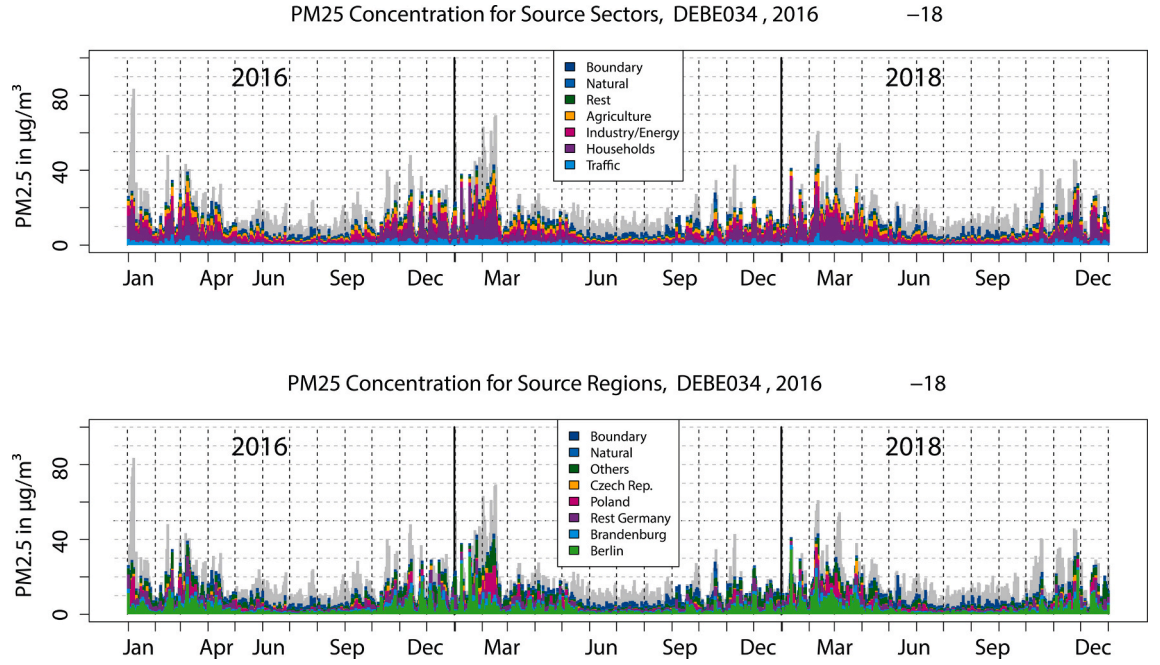

Fig. 5. Time series of the $PM_{2.5}$ mass concentration for Berlin (UB station DEBE034) for 2016 to 2018. Observations are shown in grey and modelled sector (A) and regional (B) contributions are colour coded. (For interpretation of the references to colour in this figure legend, the reader is referred to the Web version of this article.)

running mean of 7 days was applied. The observed increments are shown in solid lines, while those for the simulations are dashed (colours for each year: 2016: black; 2017: red; 2018: blue). For $PM_{2.5}$ (upper panel) the observed urban increment shows a clear seasonality with increased variability from autumn to spring with values often ranging between 5 and 10 µg/m^3. During summertime typical values are below 5 µg/m^3 and the time series shows rather limited fluctuations. Only a few periods show a negative urban increment implying that concentrations in the rural background were higher than in the urban background. A pronounced and prolonged enhancement of the urban increment was observed from mid-January to mid-February 2017 when Berlin was hit by a PM episode during stagnant easterly flow which will be further discussed below. The modelled urban increment shows lower variability than the observed and with only few exceptions underestimates the observed increment throughout the investigation period. While the model does capture the seasonal variation with higher amplitudes from autumn to spring the model underestimation is most distinct during summertime when the modelled urban increment is almost non-existent.

For the coarse mode (Fig. 7, lower panel) the seasonal signal of the observed urban increment is less pronounced than those of $PM_{2.5}$. The variability between the years is large, indicating that the variability is mainly driven by synoptic meteorological variability. An increase in variability and amplitude can be found during springtime and early autumn. Furthermore, negative urban increments of the coarse mode are more frequently observed compared to $PM_{2.5}$, illustrating sources of course material in the rural surrounding of Berlin. During the PM episode in early 2017 the coarse mode shows a negative urban increment. As expected from the large bias for the coarse mode, the modelled urban increment is almost non-existent throughout the seasons for all years which reveals a distinct discrepancy between modelled and observed increment. A potential reason for this underestimation is dust

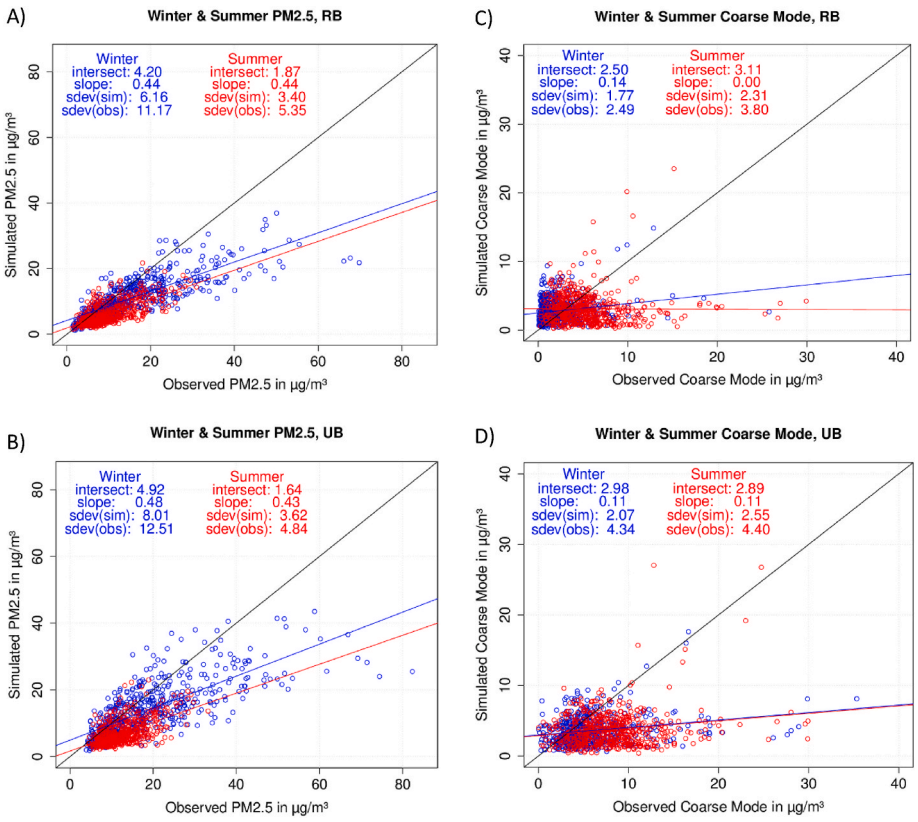

Fig. 6. Scatterplots with linear regression for 2016 to 2018 of the $PM_{2.5}$ mass concentration at rural (A) and urban (B) sites and the coarse mode fraction at rural (C) and urban (D) sites.

Table 3
Model performance statistics for all monitoring stations and the three-year period of 2016–2018. Shown are the concentrations for PM_{10}, $PM_{2.5}$ and the coarse mode fraction (PM_{CO}) for observed and modelled data: the mean values, the correlation (Pearson), the normalized RMSE (root mean squared error), the normalized BIAS (deviation of the mean). The normalization was done by dividing by the respective observational mean.

Station		Mean PM_{10}		Mean $PM_{2.5}$		Mean PM_{CO}		Correlation			Normalized RMSE			Normalized BIAS		
No.	site	OBS	SIM	OBS	SIM	OBS	SIM	PM_{10}	$PM_{2.5}$	PM_{CO}	PM_{10}	$PM_{2.5}$	PM_{CO}	PM_{10}	$PM_{2.5}$	PM_{CO}
DEBB053	RB	17.54	11.68	13.32	8.75	4.23	2.93	0.58	0.80	0.08	0.62	0.58	1.30	−0.33	−0.34	−0.31
DEBB065	RB	14.85	11.52	11.42	8.57	3.42	2.96	0.68	0.81	0.12	0.52	0.52	0.92	−0.22	−0.25	−0.13
DEBE010	UB	20.73	13.07	14.95	9.52	5.91	3.55	0.69	0.78	0.13	0.3	0.69	0.93	−0.37	−0.44	−0.40
DEBE034	UB	22.89	14.18	16.10	10.60	6.91	3.58	0.61	0.75	0.15	0.55	0.54	1.00	−0.38	−0.33	−0.48
DEBE068	UB	22.03	14.96	15.47	11.01	6.69	3.95	0.59	0.72	0.17	0.53	0.52	0.96	−0.32	−0.28	−0.41

resuspension, which will be discussed below.

3.3. Source attribution for particulate matter in Berlin

Although the model systematically underestimates the observed $PM_{2.5}$ (and PM_{10}) levels, in this section we present a sectoral and regional source attribution for $PM_{2.5}$ and PM_{10} of the Berlin agglomeration area. Since the episodes with the highest particulate matter concentrations occur during the fine mode dominated cold season and the model performance is best for $PM_{2.5}$, our main focus is on the source attribution of $PM_{2.5}$. The sectoral/regional source attribution provides insights to the most important source sectors/regions contributing to Berlin's PM mass concentration.

An overview of the annual mean contributions of source sectors and regions for Berlin and the rural background is also presented in Table 4. For Berlin the (3 year-) mean modelled urban background $PM_{2.5}$ concentrations for the 2016 to 2018 (10.4 µg/m^3) are explained by households (3.2 µg/m^3), industry & energy (2.0 µg/m^3), boundary (1.4 µg/m^3), agriculture (1.3 µg/m^3), traffic (1.3 µg/m^3), rest (0.7 µg/m^3) and natural (0.5 µg/m^3). The modelled annual mean urban increment for $PM_{2.5}$ is mainly composed of households (1.6 µg/m^3) and traffic (0.5 µg/m^3). During the whole period the most important contribution to PM_{CO} comes from (semi-)natural sources, i.e., sea salt and dust. In the rural background natural sources contribute 1.6 µg/m^3 on average to PM_{CO}. Agriculture provides a secondary contribution in the rural background, whereas in the urban background the traffic contribution (0.8 µg/m^3) is the second largest source sector. The modelled traffic contribution in the city is largely due to urban traffic as the modelled traffic increment is 0.55 µg/m^3. The remaining sectors only show small modelled increments (± 0.1 µg/m^3) for PM_{CO}. As $PM_{2.5}$ is a large fraction of PM_{10}, the PM_{10} source attribution looks similar to $PM_{2.5}$ throughout the year with respect to the relative shares, but with enhanced natural contribution derived from the coarse mode. The sectors contributing to rural background PM_{10} during winter show on average a fairly even distribution over the sectors industry & energy (2.9 µg/m^3), household (2.7 µg/m^3), agriculture (2.1 µg/m^3) and natural (2.0 µg/m^3) and slightly lower contributions from traffic (1.4 µg/m^3). Remaining sources play a minor role. The PM_{10} urban increment combines the $PM_{2.5}$ and coarse mode contributions from households (winter: 2.5 µg/m^3) and traffic (winter: 1.0 µg/m^3).

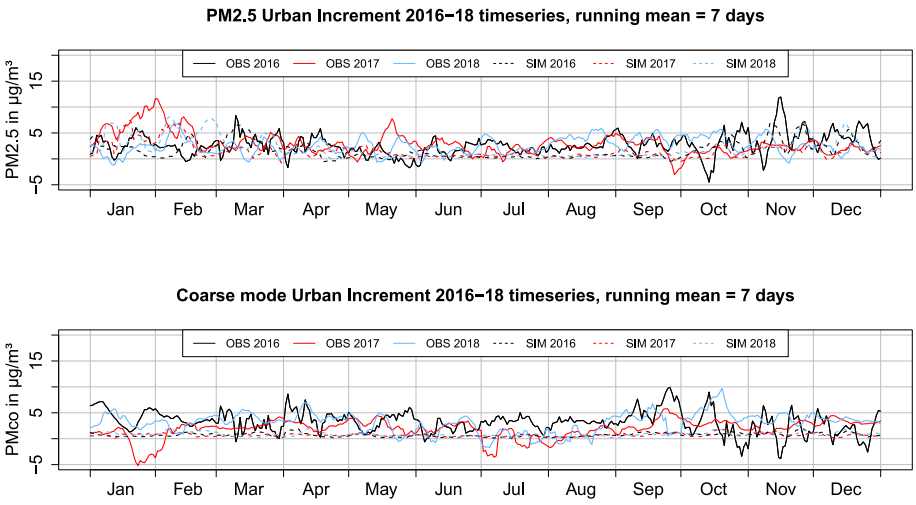

Fig. 7. Timeseries of the $PM_{2.5}$ (upper panel) and coarse mode (lower panel) urban increments for 2016–2018. The observed and modelled data were smoothed by using a 7-day running mean.

Table 4
Mean labelled concentrations for sectors and regions for $PM_{2.5}$ and PM_{CO} for RB, UB and the urban increment.

Source	Label	UB (µg/m³)		RB (µg/m³)		Urban Increment (µg/m³)	
		$PM_{2.5}$	PM_{CO}	$PM_{2.5}$	PM_{CO}	$PM_{2.5}$	PM_{CO}
Sector	Traffic	1.25	0.77	0.90	0.22	0.35	0.55
	Housholds	3.21	0.05	1.67	0.02	1.54	0.04
	Industry &En.	2.01	0.31	2.05	0.29	−0.03	0.02
	Agriculture	1.25	0.38	1.38	0.45	−0.14	−0.07
	Rest	0.74	0.20	0.70	0.12	0.04	0.08
	Natural	0.54	1.68	0.56	1.56	−0.02	0.11
	Boundary	1.38	0.30	1.40	0.28	−0.02	0.02
	Sum:	10.38	3.69	8.66	2.95	1.72	0.75
Region	Berlin	2.62	0.78	0.31	0.06	2.31	0.72
	Brandenburg	0.68	0.13	0.92	0.16	−0.25	−0.03
	Rest Ger.	1.80	0.41	2.03	0.52	−0.23	−0.11
	Poland	0.95	0.08	0.96	0.07	−0.01	0.01
	Czech Rep.	0.25	0.02	0.25	0.02	0.00	0.00
	Others	2.15	0.29	2.22	0.27	−0.07	0.02
	Natural	0.54	1.68	0.56	1.56	−0.02	0.11
	Boundary	1.38	0.30	1.40	0.28	−0.02	0.02
	Sum:	10.38	3.69	8.66	2.95	1.72	0.75

From a geographical perspective the main source area for the $PM_{2.5}$ in Berlin is Germany (5.1 µg/m³) itself, followed by the contributions from transboundary transport (3.4 µg/m³). The German contributions can be separated into Berlin (2.6 µg/m³), Brandenburg (0.7 µg/m³) and remaining states of Germany (1.8 µg/m³), which reveals that on average the city contribution slightly exceeds the contribution of the remaining German sources. The modelled contribution from foreign countries to the urban background is about as large as that of Berlin and Brandenburg combined. On average, the transboundary contribution exceeds those of domestic contribution in air masses advected to Berlin. Note that Berlin also contributes to the average rural background (~0.4 µg/m³). About one third of foreign shares can be attributed to Germany's neighbouring countries Poland (1 µg/m³) and Czech Republic (0.3 µg/m³). The remaining foreign contribution (2.2 µg/m³) strongly correlate to the contributions of Poland and Czech Republic, highlighting the importance of transport of PM from further (south-)east. Throughout the year the geographic origin remains similar in terms of relative contributions.

For PM_{CO} the importance of long-range transport is lower. The modelled contribution of German sources exceeds those of the transboundary contribution, which is explained by the shorter lifetime of the coarse mode. The coarse mode fraction in the RB has largest contributions from natural (1.6 µg/m³) and the rest of Germany (0.5 µg/m³), while the shares of the remaining regions are forming additional 0.9 µg/m³. The geographic origin contributions for PM_{10} are very similar to that of $PM_{2.5}$ with the same observations regarding natural contributions as discussed above.

The urban increment (PM2.5, annual mean: 1.7 µg/m³) is composed of two terms: 1) a positive increment induced by emissions in Berlin (+2.3 µg/m³), and 2) a negative increment from remaining areas (−0.6 µg/m³). The negative increments mean that the absolute contribution in the rural background is larger than in the city. This can be explained by a) the deposition of PM transported into the city from outside and b) the further dilution of nearby rural emissions when entering the city. Besides the positive increments explained by households and traffic emissions there is a small increment labelled natural (~0.1 µg/m³ annual mean), which is mainly associated with sea salt in 2016 and 2017, while in 2018 it additionally contains continental dust. This natural labelled increment results rather from the configuration of the measurement locations than from an urban source since the urban stations are slightly closer to the coast.

Figs. 8 and 9 provide a graphical overview of the source apportioned rural background concentration and urban increments. The figure is separated into two panels: the upper one highlights the winter period, the lower one the summer season. The figure is split into several subfigures. In Fig. 8A and B the observational data for PM_{10}, $PM_{2.5}$ and the

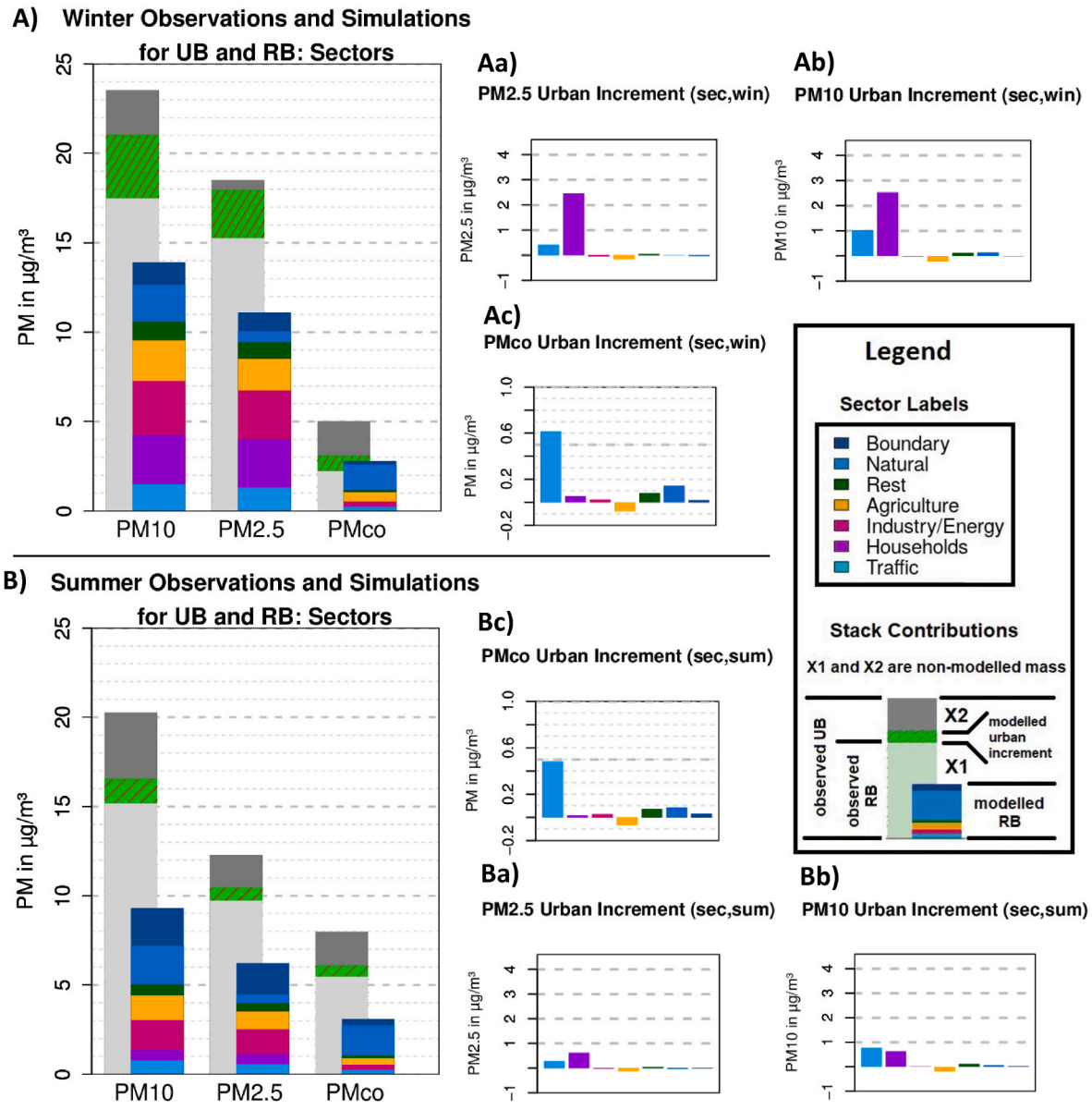

Fig. 8. Overview of observed and modelled concentrations and the increments for PM_{10}, $PM_{2.5}$ and PM_{CO} (coarse mode fraction). The observed rural background levels provided in light grey. The urban increment is provided in dark grey. As the modelled increments underestimate the observations we provide the modelled urban increment as the green hatched in this bar. The modelled RB sectors contributions are indicated in the coloured bar. The modelled urban increment is detailed per sector in the separate graphs on the right side of the figure (Aa/Ba for $PM_{2.5}$, Ab/Bb for PM_{10} and Ac/Bc for the coarse mode, A for winter and B for summer). (For interpretation of the references to colour in this figure legend, the reader is referred to the Web version of this article.)

coarse mode is provided (grey for RB and dark grey for UB locations), while the modelled urban increment with an offset relative to the observed is shown (green, hatched). In front of the observed RB, the modelled RB (colour-shaded) is shown. Since the urban increment is the difference between the urban and rural background, subfigures Aa/Ba ($PM_{2.5}$), Ab/Bb (for PM_{10}) and Ac/Bc (coarse mode) contain the increments for the absolute sector contributions. Negative contributions in the urban increment can appear (e.g., agriculture) due to larger modelled concentration outside the city than (attributed to the same sector) inside the city. The absolute contributions of the source sectors households and industry & energy show the largest variation in time. The contribution from households in the urban background dominates during the cold season (October–March) with mass concentrations of 5.2 µg/m^3, followed by industry & energy (2.7 µg/m^3), traffic (1.6 µg/m^3) and agriculture (1.4 µg/m^3). During the warm season (April–September) the order of importance shifts with larger relative contributions for e.g., industry & energy (1.5 µg/m^3). During the warm season, the absolute contribution of the remaining source sectors is roughly halved, except for households showing a fifth of their winter contributions. Hence, in summer the largest contributions for UB $PM_{2.5}$ derive from industry & energy (1.4 µg/m^3), households (1.2 µg/m^3), agriculture (0.9 µg/m^3), and traffic (0.8 µg/m^3).

The modelled timeseries allows to address the source attribution on a daily basis. Fig. 5 includes the contributions simulated by the LOTOS-EUROS CTM for source sectors (Fig. 5A) and source regions (Fig. 5B) at station BENAN representing the urban background of Berlin. The sectoral contributions contain traffic (light blue), households (purple), industry/energy (dark pink), agriculture (orange), rest (green), natural (blue) and boundary (dark blue). For the regional contributions, the labels are defined as: Berlin (light green), Brandenburg (light blue), rest of Germany (purple), Poland (dark pink), Czech Republic (orange), others (green), natural (blue) and boundary (dark blue). From day-to-

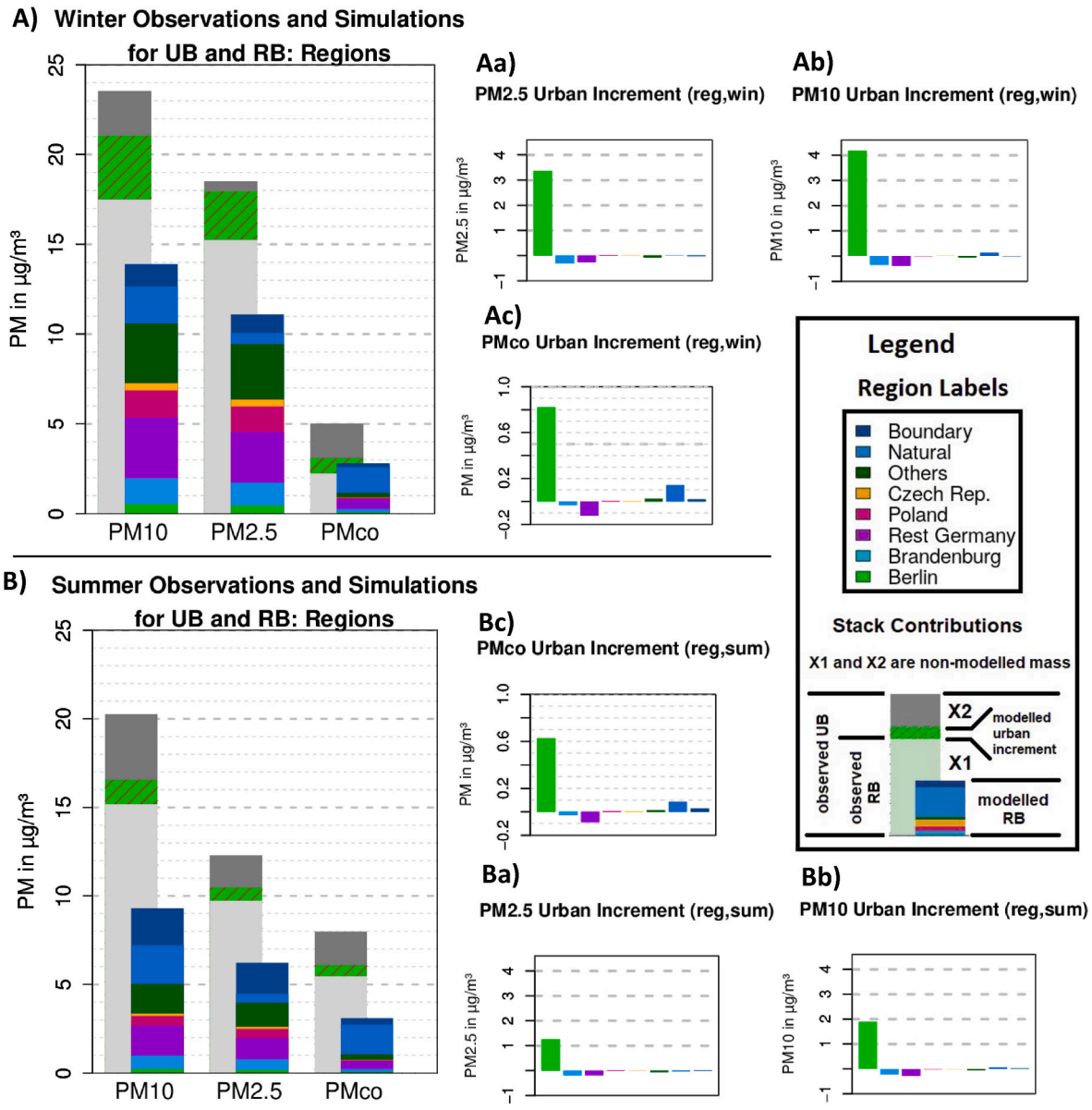

Fig. 9. Same as in Fig. 8, but for regional contributions.

day and for individual periods/episodes the (relative) source contributions and dominant sectors may differ largely from the mean. For example, during certain peaks in January 2018 the Berlin share rises up to 80%. More frequently, Poland contributes an important fraction of total $PM_{2.5}$ mass during wintertime high-concentration episodes, with contributions up to 1/3rd of the total modelled mass (e.g., January 2016, January/February 2017, or March 2018). Zooming into the situation at the beginning of 2017, the variability induced by meteorological conditions is nicely illustrated. At the beginning of the episode the model estimates high Berlin contributions for $PM_{2.5}$ (with about 34 µg/m^3) during the stagnant conditions until the weather regime changed to more diluting conditions (increased wind speeds and planetary boundary layer height). Afterwards a continental high-pressure system dominated the weather situation causing easterly flows towards Berlin. During this period the contributions from Poland, Czech Republic and remaining foreign countries (= others) take over the dominating share with a combined contribution of 2/3rd of the simulated mass. During this phase the energy/industry contribution is relatively enlarged as well, although households remain the most important sector. The episode lasted until mid-February when a trough took over control of the weather causing the transport of maritime air from the north Atlantic towards Berlin. As a result, the contributions from Poland, Czech Republic and others diminished and contributions from German sources dominated the picture again.

4. Discussion and conclusion

In this paper we conducted an air pollution simulation with the LOTOS-EUROS CTM, to address the source attribution of particulate matter (PM) for the Berlin agglomeration area as a first step towards defining the relevant brute force calculations for the determination of effectivity. The modelled timeseries allows to address the source attribution on a daily basis. The (relative) source contributions and dominant source sectors vary strongly between episodes. On average, the households and industry & power contribute the largest share to the modelled $PM_{2.5}$ levels in Berlin. Domestic contributions on average exceed those of transboundary transport, of which the city contribution slightly exceeds the contribution of the remaining German sources. During wintertime episodes the importance of source regions in Poland and further east was highlighted. The source attribution for PM_{10} looks

similar with respect to the relative shares, except that the natural contribution is enhanced compared to that in $PM_{2.5}$.

The evaluation of the model against UBA measurements has shown an overall underestimation for PM. Overall, the fine mode is better reproduced by the model than the coarse mode. The systematic underestimation of modelled PM is a feature that has been pointed out in earlier studies using LOTOS-EUROS (Weijers et al., 2010; Hendriks et al., 2013; Manders et al., 2017) and that is shared by many other chemistry transport models (Marécal et al., 2015; Bessagnet et al., 2016; Potier et al., 2019; Belis et al., 2020; Pommier et al., 2020). In previous studies the missing mass modelling $PM_{2.5}$ with LOTOS-EUROS was related to a missing share of organic carbon (OC) (Hendriks et al., 2013; Timmermans et al., 2013). This is largely solved by the inclusion of condensable material (Denier Van Der Gon et al., 2015). For a general discussion on the fine mode, we refer to abovementioned publications. Below, we mainly focus on the coarse mode and the urban increment.

The modelled coarse mode urban increment is underestimated by a factor of 4. Traffic resuspension is a well-known source of coarse mode particles in the urban atmosphere (Amato et al., 2009). A study by van Pinxteren et al. (2019) found that the combined traffic exhaust and resuspension source profile contributed 17% to urban background PM_{10} in Berlin, whereas the contribution was around 9% in the rural background. Applying these percentages to the observed 3-year mean concentrations of this study an indication of the typical urban increment (2.5 $\mu g/m^3$) for this source profile can be obtained. As the profile is dominated by crustal material and the total coarse mode increment for Berlin is about 3 $\mu g/m^3$, the traffic crustal factor obtained by van Pinxteren et al. (2019) explains the coarse mode increment to a large part. In the receptor modelling contributions from highly correlated sources may appear in the same profile (Chan et al., 1999). Hence, other urban sources may still be included into the estimate. Nevertheless, we conclude that the modelled traffic increment (0.8 $\mu g/m^3$), being much lower than deduced from the observations, explains a large part of the underestimation of the coarse mode increment.

Although there is a large body of work on modeling desert dust, little attention has been given to the modelling of crustal material from other sources in chemistry transport models. Emission inventories do not contain estimates of resuspension of e.g., traffic and land preparation, although they can be important sources (Belis et al., 2020; Denby et al., 2013; Maffia et al., 2020; Thouron et al., 2018). Most model systems do not include resuspension parameterizations for emissions from traffic and land management activities. Earlier work from Pay et al. (2011) and Schaap et al. (2009) showed that implementing a simple resuspension scheme reduced the BIAS and error in PM_{10} predictions. In our model set-up emission factors are applied to the mileage driven in each grid-cell for urban, rural and highway traffic. Implicitly, it is therefore assumed that the dust reservoir remains constant over time. Only in case of precipitation, the resuspension emission flux is set to zero. The spatial variability of the emission factors is calculated based on annual average soil water content (Schaap et al., 2009). Hence, seasonal variability as well as the impact of droughts are not included. Given the range of a factor of four in reported emission factors between regions (Gehrig et al., 2004), an impact of seasonality and especially drought periods are to be expected. In a follow-up study we plan to investigate different approaches to improve this parameterization.

Another issue that contributes to the overall underestimation of PM concentrations is the reduced capability of CTMs to model PM during stagnant weather conditions. A comparison between different CTMs showed that the models treat the vertical mixing very differently (Stern et al., 2008). A recent study connecting LOTOS-EUROS to an ensemble of COSMO-CLM simulations with different parameterizations for boundary layer meteorology, however, did not show a systematic effect of different schemes (Thürkow et al., 2021). Currently, the LOTOS-EUROS team is assessing the possibility to move away from the mixed-boundary layer concept to a set-up with a significantly larger number of layers, which has shown to give improved temporal behavior of the major air pollutants including PM (Escudero et al., 2019; Thürkow et al., 2021).

The use of national scale emission inventories may also lead to problems due to the use of proxy data, such as population density. For instance, using population density to spatially distribute emissions neglects that urban populations are much more energy efficient than rural populations (Lobo et al., 2009; Timmermans et al., 2013). Such assumptions may lead to systematic over and underestimations of urban emissions in downscaled emission inventories, as for example shown for residential heating emissions in Paris (Timmermans et al., 2013). In this study for Berlin, we also used a national scale emission inventory, and clearly underestimate the urban increment. For NO_x Kuik et al. (2018) have shown that the emission totals of the national scale and local inventory for Berlin were only a few percent apart. In their study, Kuik et al. (2018) concluded that the large systematic BIAS between WRF-CHEM modelled and observed NO_2 levels was connected to a general underestimation of NO_x emissions from traffic. Hence, primary emissions of transport need future attention. To improve the temporal and spatial variability of emissions from the residential heating sector we have applied temperature dependent emissions as this leads to improved modelled pollutant concentrations (Mues et al., 2014). Similarly, dynamic approaches should also be included for other sectors like e.g., road transport, which also shows considerable variability due to ambient temperature (Matzer et al., 2017). In a follow up study, we plan to assess if these recent findings significantly affect the modelled urban increments for NO_2 and PM.

Evaluating the gradients between source regions and background levels may provide important information to get to the reason of the underestimation. We have used the traditional approach of Lenschow in this paper (Lenschow et al., 2001). Recently, using this approach to calculate the impact of a city was criticized because the rural background concentrations partly include the urban signal (Thunis, 2018). Hence the urban increment would underestimate the urban contribution. In our study the gradients between urban and rural sites were calculated in the same way for the modelled and observed results. The modelled urban contribution to the UB $PM_{2.5}$ concentration is 2.62 $\mu g/m^3$ whereas the modelled increment is 1.72 $\mu g/m^3$. Thunis (2018) used a BF approach to quantify the impact of the urban emissions on the (rural) background concentrations as function of the distance to the city for London, Paris, Berlin and Brussels using the CHIMERE model for 2010. Although the size of the urban contribution depends on the choice and configuration of the rural and urban observation sites as well as the model system used, our study confirms that the urban increment from the Lenschow approach is a lower estimate for the urban contribution in the city.

In order to reveal further shortcomings of the model system we recommend a comparison of LOTOS-EUROS results to those of receptor model results. Furthermore, a dynamic model evaluation as in Banzhaf et al. (2015) but including source attribution would help to further analyse the source attribution of the model and reveal its weaknesses. For the near future we propose the enhancement of resuspension schemes in CTMs and an improvement of the emission variability in space and time.

Code and data availability

The LOTOS-EUROS source apportionment code used in this study is property of TNO and not allowed to be shared publicly. The LOTOS-EUROS model is available as open source-version (excluding the data source attribution package) for public use via www.lotos-euros.tno.nl.

CRediT authorship contribution statement

Joscha Pültz: Conceptualization, Methodology, Software, Validation, Formal analysis, Investigation, Resources, Data curation, Writing – original draft, Writing – review & editing, Visualization. **Sabine**

Banzhaf: Software, Writing – review & editing, Supervision. **Markus Thürkow:** Conceptualization, Methodology, Software, Resources, Writing – review & editing. **Richard Kranenburg:** Software, Resources. **Martijn Schaap:** Conceptualization, Methodology, Software, Writing – review & editing, Supervision, Project administration, Funding acquisition.

Declaration of competing interest

The authors declare that they have no known competing financial interests or personal relationships that could have appeared to influence the work reported in this paper.

Data availability

The data used in this article is partly publicly available and partly produced by own simulations. The data/code from the simulations is partly confidential. Data will be made available on request.

Acknowledgments

This research was funded by the Federal Ministry of Transport and Digital Infrastructure (BMVI) within the framework of the mFUND research initiative (grant no. 19F2065). It was partly supported by the Senat of Berlin and the Umweltbundesamt (UBA), which provided data. And finally, to the HPC Service of ZEDAT, Freie Universität Berlin, for computing time (Bennett et al., 2020), the R Core Team (2014) for the provision of software and Mr. Bergmann, for his support in setting up the computational environment.

References

Amato, F., Pandolfi, M., Escrig, A., Querol, X., Alastuey, A., Pey, J., Perez, N., Hopke, P. K., 2009. Quantifying road dust resuspension in urban environment by Multilinear Engine: a comparison with PMF2. Atmos. Environ. 43 (17), 2770–2780. https://doi.org/10.1016/j.atmosenv.2009.02.039.

Baklanov, A., Schlünzen, K., Suppan, P., Baldasano, J., Brunner, D., Aksoyoglu, S., Carmichael, G., Douros, J., Flemming, J., Forkel, R., Galmarini, S., Gauss, M., Grell, G., Hirtl, M., Joffre, S., Jorba, O., Kaas, E., Kaasik, M., Kallos, G., et al., 2014. Online coupled regional meteorology chemistry models in Europe: current status and prospects. Atmos. Chem. Phys. 14 (1), 317–398. https://doi.org/10.5194/acp-14-317-2014.

Banzhaf, S., Schaap, M., Kerschbaumer, A., Reimer, E., Stern, R., van der Swaluw, E., Builtjes, P., 2012. Implementation and evaluation of pH-dependent cloud chemistry and wet deposition in the chemical transport model REM-Calgrid. Atmos. Environ. 49, 378–390. https://doi.org/10.1016/j.atmosenv.2011.10.069.

Banzhaf, S., Schaap, M., Wichink Kruit, R.J., Denier van der Gon, H.A.C., Stern, R., Builtjes, P.J.H., 2013. Impact of emission changes on secondary inorganic aerosol episodes across Germany. Atmos. Chem. Phys. 13, 11675–11693. https://doi.org/10.5194/acp-13-11675-2013.

Banzhaf, S., Schaap, M., Kranenburg, R., Manders, A.M.M., Segers, A.J., Visschedijk, A.J. H., van der Gon, H.A.C.D., Kuenen, J.J.P., van Meijgaard, E., van Ulft, L.H., Cofala, J., Builtjes, P.J.H., 2015. Dynamic model evaluation for secondary inorganic aerosol and its precursors over Europe between 1990 and 2009. In: Geoscientific Model Development, vol. 8. https://doi.org/10.5194/gmd-8-1047-2015, 4.

Beekmann, M., Prévôt, A.S.H., Drewnick, F., Sciare, J., Pandis, N., et al., 2015. In situ, satellite measurementand model evidence on the dominant regional contribution to fine particulate matter levels in theParis megacity. Atmos. Chem. Phys. Discuss. Eur. J. Geosci. Union. 15 (16), 9577–9591. https://doi.org/10.5194/acp-15-9577-2015ï, 10.5194/acp-15-9577-2015. insu-01285053.

Belis, C.A., Pernigotti, D., Pirovano, G., Favez, O., Jaffrezo, J.L., Kuenen, J., Denier van Der Gon, H., Reizer, M., Riffault, V., Alleman, L.Y., Almeida, M., Amato, F., Angyal, A., Argyropoulos, G., Bande, S., Beslic, I., Besombes, J.L., Bove, M.C., Brotto, P., et al., 2020. Evaluation of receptor and chemical transport models for PM10 source apportionment. Atmos. Environ. X, 5. https://doi.org/10.1016/j.aeaoa.2019.100053.

Bennett, L., Melchers, B., Proppe, B., 2020. Curta: A General-Purpose High-Performance Computer at ZEDAT. Freie Universität Berlin. https://doi.org/10.17169/refubium-26754.

Bessagnet, B., Pirovano, G., Mircea, M., Cuvelier, C., Aulinger, A., Calori, G., Ciarelli, G., Manders, A., Stern, R., Tsyro, S., Garciá Vivanco, M., Thunis, P., Pay, M.T., Colette, A., Couvidat, F., Meleux, F., Rouïl, L., Ung, A., Aksoyoglu, S., et al., 2016. Presentation of the EURODELTA III intercomparison exercise-evaluation of the chemistry transport models' performance on criteria pollutants and joint analysis with meteorology. Atmos. Chem. Phys. 16 (19), 12667–12701. https://doi.org/10.5194/acp-16-12667-2016.

Boldo, E., Medina, S., LeTertre, A., Hurley, F., Mücke, H.G., Ballester, F., Aguilera, I., Eilstein, D., 2006. Apheis: health impact assessment of long-term exposure to PM2.5 in 23 European cities. Eur. J. Epidemiol. 21 (6), 449–458. https://doi.org/10.1007/s10654-006-9014-0.

Brook, R.D., Rajagopalan, S., Pope, C.A., Brook, J.R., Bhatnagar, A., Diez-Roux, A.v., Holguin, F., Hong, Y., Luepker, R.v., Mittleman, M.A., Peters, A., Siscovick, D., Smith, S.C., Whitsel, L., Kaufman, J.D., 2010. Particulate matter air pollution and cardiovascular disease: an update to the scientific statement from the american heart association. In: Circulation, vol. 121, pp. 2331–2378. https://doi.org/10.1161/CIR.0b013e3181dbece1, 21.

Chan, Y.C., Simpson, R.W., Mctainsh, G.H., Vowles, P.D., Cohen, D.D., Bailey, G.M., 1999. Source apportionment of PM2.5 and PM10 aerosols in Brisbane (Australia) by receptor modelling. In: Atmospheric Environment, vol. 33.

Clappier, A., Belis, C., Pernigotti, D., Thunis, P., 2017. Source apportionment and sensitivity analysis: two methodologies with two different purposes. Geosci. Model Dev. (GMD) 10, 4245–4256.

Costa, L.G., Cole, T.B., Coburn, J., Chang, Y.C., Dao, K., Roque, P., 2014. Neurotoxicants are in the air: convergence of human, animal, and in vitro studies on the effects of air pollution on the brain. In: BioMed Research International. https://doi.org/10.1155/2014/736385.

Curier, R.L., Kranenburg, R., Segers, A.J.S., Timmermans, R.M.A., Schaap, M., 2014. Synergistic use of OMI NO2 tropospheric columns and LOTOS-EUROS to evaluate the NOx emission trends across Europe. Rem. Sens. Environ. 149 https://doi.org/10.1016/j.rse.2014.03.032.

Denby, B.R., Sundvor, I., Johansson, C., Pirjola, L., Ketzel, M., Norman, M., Kupiainen, K., Gustafsson, M., Blomqvist, G., Omstedt, G., 2013. A coupled road dust and surface moisture model to predict non-exhaust road traffic induced particle emissions (NORTRIP). Part 1: road dust loading and suspension modelling. Atmos. Environ. 77, 283–300. https://doi.org/10.1016/j.atmosenv.2013.04.069.

Denier Van Der Gon, H.A.C., Bergström, R., Fountoukis, C., Johansson, C., Pandis, S.N., Simpson, D., Visschedijk, A.J.H., 2015. Particulate emissions from residential wood combustion in Europe - revised estimates and an evaluation. Atmos. Chem. Phys. 15 (11), 6503–6519. https://doi.org/10.5194/acp-15-6503-2015.

Deutscher Wetterdienst, 2020. Klimastatusbericht deutschland jahr 2018. Deutscher Wetterdienst Bildungszentrum. https://www.dwd.de/DE/leistungen/klimastatusbericht/publikationen/ksb_2018.pdf?_blob=publicationFile&v=5.

Dunker, A.M., Yarwood, G., Ortmann, J.P., Wilson, G.M., 2002. The decoupled direct method for sensitivity analysis in a three-dimensional air quality model - implementation, accuracy, and efficiency. Environ. Sci. Technol. 36, 2965–2976. https://doi.org/10.1021/es0112691.

Escudero, M., Segers, A., Kranenburg, R., Querol, X., Alastuey, A., Borge, R., de La Paz, D., Gangoiti, G., Schaap, M., 2019. Analysis of summer O3 in the Madrid air basin with the LOTOS-EUROS chemical transport model. Atmos. Chem. Phys. 19 (22), 14211–14232. https://doi.org/10.5194/acp-19-14211-2019.

Fountoukis, C., Nenes, A., 2007. ISORROPIAII: a computationally efficient thermodynamic equilibrium model for K+-Ca2+-Mg2+-NH4+-Na+-SO42–NO3–Cl–H2O aerosols. Atmos. Chem. Phys. 7 (17) https://doi.org/10.5194/acp-7-4639-2007.

Fuzzi, S., Baltensperger, U., Carslaw, K., Decesari, S., Denier Van Der Gon, H., Facchini, M.C., Fowler, D., Koren, I., Langford, B., Fuzzi, S., Baltensperger, U., Carslaw, K., Decesari, S., Denier Van Der Gon, H., Facchini, M.C., Fowler, D., Koren, I., Langford, B., Lohmann, U., et al., 2015. Particulate matter, air quality and climate: lessons learned and future needs ETH Library Particulate matter, air quality and climate: lessons learned and future needs. Atmos. Chem. Phys. 15 (14), 8217–8299. https://doi.org/10.3929/ethz-b-000103253.

Gehrig, R., Hill, M., Buchmann, B., Imhof, D., Weingartner, E., Baltensperger, U., 2004. Separate determination of PM10 emission factors of road traffic for tailpipe emissions and emissions from abrasion and resuspension processes. Int. J. Environ. Pollut. 22 (3) https://doi.org/10.1504/IJEP.2004.005549.

Hendriks, C., Kranenburg, R., Kuenen, J., van Gijlswijk, R., Wichink Kruit, R., Segers, A., Denier van der Gon, H., Schaap, M., 2013. The origin of ambient particulate matter concentrations in The Netherlands. Atmos. Environ. 69, 289–303. https://doi.org/10.1016/j.atmosenv.2012.12.017.

Hendriks, C., Kuenen, J., Kranenburg, R., Scholz, Y., Schaap, M., 2015. A shift in emission time profiles of fossil fuel combustion due to energy transitions impacts source receptor matrices for air quality. Environ. Sci. J. Integr. Environ. Res.: Process. Impacts 17 (3), 510–524. https://doi.org/10.1039/c4em00444b.

Kaiser, J.W., Heil, A., Andreae, M.O., Benedetti, A., Chubarova, N., Jones, L., Morcrette, J.J., Razinger, M., Schultz, M.G., Suttie, M., van der Werf, G.R., 2012. Biomass burning emissions estimated with a global fire assimilation system based on observed fire radiative power. In: Biogeosciences, vol. 9, pp. 527–554. https://doi.org/10.5194/bg-9-527-2012, 1.

Kranenburg, R., Schaap, M., Huibregtse, E., Hendriks, C., Segers, A., 2013a. Source apportionment in the LOTOS-EUROS air quality model. NATO Sci. Peace Secur. Ser C: Environ. Secur. 137 https://doi.org/10.1007/978-94-007-5577-2_65.

Kranenburg, R., Segers, A.J., Hendriks, C., Schaap, M., 2013b. Source apportionment using LOTOS-EUROS: module description and evaluation. Geosci. Model Dev. (GMD) 6 (3), 721–733. https://doi.org/10.5194/gmd-6-721-2013.

Kuik, F., Kerschbaumer, A., Lauer, A., Lupascu, A., von Schneidemesser, E., Butler, T.M., 2018. Top-down quantification of NOx emissions from traffic in an urban area using a high-resolution regional atmospheric chemistry model. Atmos. Chem. Phys. 18 (11), 8203–8225. https://doi.org/10.5194/acp-18-8203-2018.

Lenschow, P., Abraham, H., Kutzner, K., Lutz, M., Preu, J., Reichenbacher, W., 2001. Some Ideas about the Sources of PM10. Atmospheric Environment.

Li, G., Bei, N., Zavala, M., Molina, L.T., 2014. Ozone formation along the California-Mexican border region during Cal-Mex 2010 field campaign. Atmos. Environ. 88, 370–389. https://doi.org/10.1016/j.atmosenv.2013.11.067.

Lobo, J., Strumsky, D., Bettencourt, L., 2009. Metropolitan Areas and CO2 Emissions: Large Is Beautiful, Working Paper Series: Martin Prosperity Institute REF. 2009-MPIWP-006.

Maffia, J., Dinuccio, E., Amon, B., Balsari, P., 2020. PM emissions from open field crop management: emission factors, assessment methods and mitigation measures – a review. In: Atmospheric Environment, vol. 226. https://doi.org/10.1016/j.atmosenv.2020.117381.

Manders, A.M.M., Builtjes, P.J.H., Curier, L., vander, Gon.H.A., Hendriks, C., Jonkers, S., Kranenburg, R., Kuenen, J.J.P., Segers, A.J., Timmermans, R.M.A., Visschedijk, A.J.H., Kruit, R.J.W., Pul, W.A.J.V., Sauter, F.J., van der Swaluw, E., Swart, D.P.J., Douros, J., Eskes, H., van Meijgaard, E., et al., 2017. Curriculum vitae of the LOTOS-EUROS (v2.0) chemistry transport model. Geosci. Model Dev. (GMD) 10 (11), 4145–4173. https://doi.org/10.5194/gmd-10-4145-2017.

Marécal, V., Peuch, V.H., Andersson, C., Andersson, S., Arteta, J., Beekmann, M., Benedictow, A., Bergström, R., Bessagnet, B., Cansado, A., Chéroux, F., Colette, A., Coman, A., Curier, R.L., van der Gon, H.A.C.D., Drouin, A., Elbern, H., Emili, E., Engelen, R.J., et al., 2015. A regional air quality forecasting system over Europe: the MACC-II daily ensemble production. Geosci. Model Dev. (GMD) 8 (9), 2777–2813. https://doi.org/10.5194/gmd-8-2777-2015.

Mårtensson, E.M., Nilsson, E.D., de Leeuw, G., Cohen, L.H., Hansson, H.C., 2003. Laboratory simulations and parameterization of the primary marine aerosol production. J. Geophys. Res. Atmos. 108 (9) https://doi.org/10.1029/2002jd002263.

Matzer, C., Hausberger, S., Lipp, S., Rexeis, M., 2017. A new approach for systematic use of PEMS data in emission simulation. In: J. Earth Sci. Geotech. Eng, vol. 7. Scienpress Ltd, 1, online.

Monahan, E.C., Spiel, D.E., Davidson, K.L., 1986. Model of marine aerosol generation via whitecaps and wave disruption. https://doi.org/10.1007/978-94-009-4668-2_16.

Mues, A., Manders, A., Schaap, M., Kerschbaumer, A., Stern, R., Builtjes, P., 2012. Impact of the extreme meteorological conditions during the summer 2003 in Europe on particulate matter concentrations. Atmos. Environ. 55, 377–391. https://doi.org/10.1016/j.atmosenv.2012.03.002.

Mues, A., Kuenen, J., Hendriks, C., Manders, A., Segers, A., Scholz, Y., Hueglin, C., Builtjes, P., Schaap, M., 2014. Sensitivity of air pollution simulations with LOTOS-EUROS to the temporal distribution of anthropogenic emissions. Atmos. Chem. Phys. 14 (2), 939–955. https://doi.org/10.5194/acp-14-939-2014.

Napelenok, S.L., Cohan, D.S., Hu, Y., Russell, A.G., 2006. Decoupled direct 3D sensitivity analysis for particulate matter (DDM-3D/PM). Atmos. Environ. 40, 6112–6121. https://doi.org/10.1016/J.ATMOSENV.2006.05.039.

Newby, D.E., Mannucci, P.M., Tell, G.S., Baccarelli, A.A., Brook, R.D., Donaldson, K., Forastiere, F., Franchini, M., Franco, O.H., Graham, I., Hoek, G., Hoffmann, B., Hoylaerts, M.F., Künzli, N., Mills, N., Pekkanen, J., Peters, A., Piepoli, M.F., Rajagopalan, S., Storey, R.F., 2015. Expert position paper on air pollution and cardiovascular disease. In: European Heart Journal, vol. 36. Oxford University Press, pp. 83–93. https://doi.org/10.1093/eurheartj/ehu458, 2,.

Pandolfi, M., Mooibroek, D., Hopke, P., Van Pinxteren, D., Querol, X., Herrmann, H., Alastuey, A., Favez, O., Hüglin, C., Perdrix, E., Riffault, V., Sauvage, S., Van Der Swaluw, E., Tarasova, O., Colette, A., 2020. Long-range and local air pollution: what can we learn from chemical speciation of particulate matter at paired sites? Atmos. Chem. Phys. 20, 409–429. https://doi.org/10.5194/acp-20-409-2020.

Pay, M.T., Jiménez-Guerrero, P., Baldasano, J.M., 2011. Implementation of resuspension from paved roads for the improvement of CALIOPE air quality system in Spain. Atmos. Environ. 45 (3) https://doi.org/10.1016/j.atmosenv.2010.10.032.

Pommier, M., Fagerli, H., Schulz, M., Valdebenito, A., Kranenburg, R., Schaap, M., 2020. Prediction of source contributions to urban background PM10 concentrations in European cities: a case study for an episode in December 2016 using EMEP/MSC-W rv4.15 and LOTOS-EUROS v2.0 - Part 1: the country contributions. Geosci. Model Dev. (GMD) 13 (4), 1787–1807. https://doi.org/10.5194/gmd-13-1787-2020.

Potier, E., Waked, A., Bourin, A., Minvielle, F., Péré, J.C., Perdrix, E., Michoud, V., Riffault, V., Alleman, L.Y., Sauvage, S., 2019. Characterizing the regional contribution to PM 10 pollution over northern France using two complementary approaches: chemistry transport and trajectory-based receptor models. Atmos. Res. 223, 1–14. https://doi.org/10.1016/j.atmosres.2019.03.002.

Putaud, J.P., Raes, F., van Dingenen, R., Brüggemann, E., Facchini, M.C., Decesari, S., Fuzzi, S., Gehrig, R., Hüglin, C., Laj, P., Lorbeer, G., Maenhaut, W., Mihalopoulos, N., Müller, K., Querol, X., Rodriguez, S., Schneider, J., Spindler, G., ten Brink, H., Tørseth, K., Wiedensohler, A., 2004. A European aerosol phenomenology - 2: chemical characteristics of particulate matter at kerbside, urban, rural and background sites in Europe. Atmos. Environ. 38 (16) https://doi.org/10.1016/j.atmosenv.2004.01.041.

Querol, X., Alastuey, A., Ruiz, C.R., Artiñano, B., Hansson, H.C., Harrison, R.M., Buringh, E., ten Brink, H.M., Lutz, M., Bruckmann, P., Straehl, P., Schneider, J., 2004. Speciation and origin of PM10 and PM2.5 in selected European cities. Atmos. Environ. 38 (38) https://doi.org/10.1016/j.atmosenv.2004.08.037.

R Core Team, 2014. R: A Language and Environment for Statistical Computing. R Foundation for Statistical Computing, Vienna, Austria. URL. http://www.R-project.org/.

Schaap, M., Manders, A., Hendriks, E., Cnossen, J., Segers, A., Denier van der Gon, H., Jozwicka, M., Sauter, F., Velders, G., Matthijsen, J., Builtjes, P., 2009. Regional Modelling of Particulate Matter for the Netherlands.

Schaap, M., Kranenburg, R., Curier, L., Jozwicka, M., Dammers, E., Timmermans, R., 2013. Assessing the sensitivity of the OMI-NO2 product to emission changes across europe. Rem. Sens. 5 (9) https://doi.org/10.3390/rs5094187.

Schneider, C., Pelzer, M., Toenges-Schuller, N., Nacken, M., Niederau, A., 2016. ArcGIS basierte Lösung zur detaillierten, deutsch-landweiten Verteilung (Gridding) nationaler Emissionsjahreswerte auf Basis des Inventars zur Emissionsberichterstattung Langfassung.

Stern, R., Builtjes, P., Schaap, M., Timmermans, R., Vautard, R., Hodzic, A., Memmesheimer, M., Feldmann, H., Renner, E., Wolke, R., Kerschbaumer, A., 2008. A model inter-comparison study focussing on episodes with elevated PM10 concentrations. Atmos. Environ. 42 (19), 4567–4588. https://doi.org/10.1016/j.atmosenv.2008.01.068.

Thouron, L., Seigneur, C., Kim, Y., Mahé, F., André, M., Bruge, B., Chanut, H., Pellan, Y., 2018. Intercomparison of three modeling approaches for traffic-related road dust resuspension using two experimental data. Transport. Res. Transport Environ. 58 https://doi.org/10.1016/j.trd.2017.11.003.

Thunis, P., 2018. On the validity of the incremental approach to estimate the impact of cities on air quality. Atmos. Environ. 173, 210–222. https://doi.org/10.1016/j.atmosenv.2017.11.012.

Thunis, P., Clappier, A., Pisoni, E., Degraeuwe, B., 2015. Quantification of non-linearities as a function of time averaging in regionalair quality modeling applications, Atmos. Environ. Times 103, 263–275.

Thunis, P., Clappier, A., Tarrason, L., Cuvelier, C., Monteiro, A., Pisoni, E., Wesseling, J., Belis, C.A., Pirovano, G., Janssen, S., Guerreiro, C., Peduzzi, E., 2019. Source apportionment to support air quality planning: strengths and weaknesses of existing approaches. Environ. Int. 130, 104825.

Thunis, P., Clappier, A., With, G., Pisoni, E., Guerreiro, C., Dupont, A., Riffaut, H., Waersted, V., Gilardoni, J., Eriksson, S., Angyal, A., Bonafe, A., Montanari, G., 2020. Source apportionment to support air quality management practices A fitness-for-purpose guide. *V 3.1*. https://doi.org/10.2760/47145.

Thürkow, M., Kirchner, I., Kranenburg, R., Timmermans, R.M.A., Schaap, M., 2021. A multi-meteorological comparison for episodes of PM10 concentrations in the Berlin agglomeration area in Germany with the LOTOS-EUROS CTM. Atmos. Environ. 244 https://doi.org/10.1016/j.atmosenv.2020.117946.

Thürkow, M., Banzhaf, S., Butler, T., Pültz, J., Schaap, M., 2022. Source attribution of nitrogen oxides across Germany: Comparing the labelling approach and brute force technique with LOTOS-EUROS. Atmos. Environ. https://doi.org/10.1016/j.atmosenv.2022.119412. In press.

Timmermans, R.M.A., Denier van der Gon, H.A.C., Kuenen, J.J.P., Segers, A.J., Honoré, C., Perrussel, O., Builtjes, P.J.H., Schaap, M., 2013. Quantification of the urban air pollution increment and its dependency on the use of down-scaled and bottom-up city emission inventories. Urban Clim. 6, 44–62. https://doi.org/10.1016/j.uclim.2013.10.004.

Timmermans, R., Kranenburg, R., Manders, A., Hendriks, C., Segers, A., Dammers, E., Denier van der Gon, H., Schaap, M., Dammers, E., Zeng, L., Wang, L., Liu, Z., 2017. Source apportionment of PM2.5 across China using LOTOS-EUROS. Atmos. Environ. 164, 370–386. https://doi.org/10.1016/j.atmosenv.2017.06.003.

Timmermans, R., Kranenburg, R., Hendriks, C., Thürkow, M., Kirchner, I., van Pinxteren, D., Schaap, M., 2020. Establishing the Origin of Particulate Matter in Eastern Germany Using an Improved Regional Modelling Framework. Springer Proceedings in Complexity. https://doi.org/10.1007/978-3-030-22055-6_1.

Umweltbundesamt, 2019. Luftqualität 2018. Vorläufige Auswertung. https://www.umweltbundesamt.de/publikationen/luftqualitaet-2018.

van Pinxteren, D., Mothes, F., Spindler, G., Fomba, K.W., Herrmann, H., 2019. Trans-boundary PM10: quantifying impact and sources during winter 2016/17 in eastern Germany. Atmos. Environ. 200, 119–130. https://doi.org/10.1016/j.atmosenv.2018.11.061.

Viana, M., Kuhlbusch, T.A.J., Querol, X., Alastuey, A., Harrison, R.M., Hopke, P.K., Winiwarter, W., Vallius, M., Szidat, S., Prévôt, A.S.H., Hueglin, C., Bloemen, H., Wåhlin, P., Vecchi, R., Miranda, A.I., Kasper-Giebl, A., Maenhaut, W., Hitzenberger, R., 2008. Source apportionment of particulate matter in Europe: a review of methods and results. In: Journal of Aerosol Science, vol. 39. Elsevier Ltd, pp. 827–849. https://doi.org/10.1016/j.jaerosci.2008.05.007, 10.

Weijers, E.P., Sahan, E., ten Brink, H.M., Schaap, M., Matthijsen, J., Otjes, R.P., van Arkel, F., 2010. Contribution of Secondary Inorganic Aerosols to PM10 and PM2.5 in the Netherlands; Measurement and Modelling Results.

Whitten, G.Z., Hogo, H., Killus, J.P., 1980. The carbon-bond mechanism: a condensed kinetic mechanism for photochemical smog. Environ. Sci. Technol. 14 (6) https://doi.org/10.1021/es60166a008.

Wichink Kruit, R.J., Schaap, M., Sauter, F.J., van Zanten, M.C., van Pul, W.A.J., 2012. Modeling the distribution of ammonia across Europe including bi-directional surface-atmosphere exchange. Biogeosciences 9 (12), 5261–5277. https://doi.org/10.5194/bg-9-5261-2012.

World Health Organization Regional Office for Europe, 2015. Economic cost of the health impact of air pollution in Europe Clean air , health and wealth. http://www.euro.who.int/pubrequest.

Zhang, L., Gong, S., Padro, J., Barrie, L., 2001. A size-segregated particle dry deposition scheme for an atmospheric aerosol module. Atmos. Environ. 35 (3) https://doi.org/10.1016/S1352-2310(00)00326-5.

Zhang, W., Capps, S.L., Hu, Y., Nenes, A., Napelenok, S.L., Russell, A.G., 2012. Development of the high-order decoupled direct method in three dimensions for particulate matter: enabling advanced sensitivity analysis in air quality models. Geosci. Model Dev. (GMD) 5, 355–368. https://doi.org/10.5194/gmd-5-355-2012.